

## FLUCTUATION SPECTRA OF WIND VELOCITY MEASURED WITH A DOPPLER LIDAR

V.A. Banakh, Ch. Werner, F. Kopp, and I.N. Smalikho

*Institute of Atmospheric Optics,  
Siberian Branch of the Russian Academy of Sciences, Tomsk, Russia  
DLR, Institute for Optoelectronics Oberpfaffenhofen, Germany  
Received December 10, 1996*

*This paper presents some results of theoretical and experimental study of the temporal spectra of fluctuations of wind velocity measured with a cw Doppler lidar. It is shown, that the temporal spectrum of wind velocity measured with a Doppler lidar essentially differs from the Kolmogorov-Obukhov's spectrum which describes turbulence of wind velocity measured at a fixed point due to low-frequency spatial filtration of wind velocity fluctuations over scattering volume. In particular, it is revealed, that when the lidar scattering volume is large and sufficiently strong side wind takes place, so that the Taylor's hypothesis of "frozen" turbulence is applicable within the probing volume, the lidar spectrum has a power frequency dependence with the power index  $-8/3$  but not  $-5/3$  as it takes place in point measurements. When the Taylor's hypothesis is not applicable, the lidar spectra have a power frequency dependence with power index approximately  $-2$ .*

### INTRODUCTION

To study dynamic processes occurring in the Earth's atmosphere it seems promising to use remote sensing methods, in particular, with Doppler (coherent) lidars. Doppler lidars developed at present are used to study both mesa-scale and turbulent variations of wind velocity field in the boundary layer and free atmosphere.<sup>1-12</sup> The principle of velocity measurements with this lidar is that the laser radiation scattered backward by aerosol particles which are completely entrained by the air flow, is collected by a receiving-transmitting telescope of lidar and detected using a coherent method. Taking into account the Doppler relation  $V = (\lambda/2)f$ , where  $V$  is the velocity,  $\lambda$  is the wavelength of a laser beam,  $f$  is the frequency, the power spectrum is a distribution by particle velocities within the volume sounded. The power spectrum is estimated from the signal recorded during a finite period. After that an estimate of the mean velocity (i.e. velocity averaged over lidar volume) is obtained from the Doppler spectrum by some way.

Doppler lidars are used to determine parameters of the dynamic turbulence as well as to measure the mean velocity.<sup>6-12</sup> In this case such characteristics as Doppler spectrum width, temporal and spatial structure functions and temporal spectra of velocity measured with a lidar bear the information. In contrast to point and small-inertial meters to analyze structure functions and velocity spectra obtained from the lidar data a problem arises of the account for spatial averaging over the volume sounded. It becomes especially urgent in

the case of large sounding paths when the volume size begins to exceed the outer scale of turbulence. The present paper is devoted to study of the spectra of wind velocity measured with a ground based cw Doppler lidar for various size of the volume sounded.

### THEORY

The sounding laser beam of a ground based cw Doppler lidar is assumed to be directed at an angle  $\varphi$  to the Earth's surface and focused at a given distance from the lidar. Radiation scattered by particles within the cross section area of the sounding beam comes at the receiving telescope of the lidar. But the principal contribution in the lidar signal is caused by the particles concentrated in the focus area.<sup>13,14</sup> The efficient longitudinal size of this area is determined by the diffraction length  $ka_0^2$ , where  $k = 2\pi/\lambda$ ;  $a_0$  is the beam radius at the telescope output and focal length  $R$ . Thus, changing  $\varphi$ ,  $R$  and  $a_0$  one can set a height of wind velocity sounding and spatial resolution of the data thus acquired.

An estimate of the wind velocity  $V_D$  is assumed to be a "centroid" of the Doppler spectrum distribution. In this case the expression for  $V_D$  in time  $t$  has the form<sup>5,15,16</sup>

$$V_D(t) = \frac{\int_0^{\infty} dz Q_s(z) \beta_{\pi}(z, 0, 0, t) V_z(z, 0, 0, t)}{\int_0^{\infty} dz Q_s(z) \beta_{\pi}(z, 0, 0, t)} + V_n(t), \quad (1)$$

where integration is performed along the sounding beam propagation axis (lidar is in the plane  $z = 0$ ),  $V_z(\mathbf{r}, t)$  is the radial component of the wind velocity vector  $\mathbf{V} = \{V_z, V_x, V_y\}$  (projection of the velocity vector on the axis  $z$  along the beam propagation) at the point  $\mathbf{r} = \{z, x, y\}$ ,  $\beta_\pi = \sigma\rho$  is the backscattering coefficient,  $\sigma$  is the backscattering cross-section,  $\rho$  is the particle concentration,  $V_n$  is the velocity estimate error determined by the value of the signal-to-noise ratio (a noise component of Doppler estimate of the

velocity). The function  $Q_s(z) = I(z) / \int_0^\infty dz I(z)$  in (1)

is the normalized intensity distribution  $I(z) = I(0) \times [(1 - z/R)^2 + z^2/(ka_0^2)]^{-1}$  of sounding beam along the propagation axis  $z$  and it determines a distance to the volume and its efficient size (spatial resolution of the measured wind velocity). In the near diffraction zone ( $R \ll ka_0^2$ )  $Q_s(z)$  has a maximum at the point  $z_m \approx R$  and for  $Q_s(z)$  one can write

$$Q_s(z) = \{\pi k a_0^2 [(1 - z/R)^2 + z^2/(k a_0^2)]\}^{-1}. \quad (2)$$

If to determine the efficient length of the volume  $\Delta z$  by the formula  $\Delta z = \int_0^\infty dz Q_s(z)/Q_z(R)$

then taking into account the condition  $R \ll ka_0^2$  it can be obtained that

$$\Delta z = (\lambda/2) (R^2/a_0^2). \quad (3)$$

It follows from (3) that at a constant radius of the beam  $a_0$  the efficient size of the volume increases with increasing focal length  $R$  (distance of sounding) in the longitudinal direction  $\Delta z$  proportionally to  $R^2$ .

The one sided spectral density  $S_D(f)$  of the velocity fluctuations measured with a Doppler lidar can be presented in the form

$$S_D(f) = 2 \int_{-\infty}^{+\infty} d\tau \langle V_D'(t + \tau) \rangle V_D'(t) e^{-i2\pi f \tau}, \quad (4)$$

where the angular brackets mean the ensemble averaging,  $V_D' = V_D - \langle V_D \rangle$ ,  $f \geq 0$ . Let us admit a set of assumptions and simplifications. We will neglect an inhomogeneity of the backscattering coefficient within the volume sounded and take in (1) that

$$\beta_\pi(\mathbf{r}, t) \approx \langle \beta_\pi \rangle \approx \text{const}. \quad (5)$$

The radial wind velocity  $\int_0^\infty dz Q_s(z) V_z(z, 0, 0, t)$

averaged over the volume sounded and the velocity noise component  $V_n(t)$  are assumed to be statistically

independent. The function  $V_n(t)$  is a delta correlated random process (the "white" noise) with the zero mean value ( $\langle V_n \rangle = 0$ ):

$$\langle V_n(t + \tau) V_n(t) \rangle = \frac{1}{2} S_n \delta(\tau), \quad (6)$$

where  $S_n = \text{const}$  is the spectrum of noise component of Doppler estimate of the velocity,  $\delta(\tau)$  is the delta function.

Analysis of the spectrum  $S_D(f)$  will be made under the assumption of stationarity, homogeneity, and isotropy of high-frequency turbulent variations of the wind velocity. Assuming that the transfer of turbulent vortices by the mean wind flow occurs without any appreciable evolution during the time of their presence within the volume sounded we use the Taylor hypothesis of the "frozen" turbulence<sup>17-19</sup>

$$V_z(z, 0, 0, t) = V_z(z - \langle V_z \rangle t, -\langle V_x \rangle t, 0, 0), \quad (7)$$

where the coordinate system is chosen in such a way that  $V_y = 0$ . As a result we have from Eqs. (1)-(7)

$$S_D(f) = 2 \int_{-\infty}^{+\infty} d\tau e^{-i2\pi f \tau} \int_0^\infty dz_1 \int_0^\infty dz_2 Q_s(z_1) Q_s(z_2) \times \\ \times B_z(z_1 - z_2 + \langle V_z \rangle \tau, \langle V_x \rangle \tau, 0) + S_n, \quad (8)$$

where  $B_z(\mathbf{r}) = \langle V_z'(\mathbf{r}' + \mathbf{r}) V_z'(\mathbf{r}') \rangle$  is the spatial correlation function of the radial component of wind velocity.

Analyzing the high-frequency spectral region  $f > |\langle \mathbf{V} \rangle|/L_V$ , where  $\langle \mathbf{V} \rangle = \{\langle V_z \rangle, \langle V_x \rangle, 0\}$ ,  $L_V$  is the outer scale of turbulence, for  $B_z(\mathbf{r})$  in Eq. (8) one can use the expression<sup>18</sup>

$$B_z(\mathbf{r}) = \int_{-\infty}^\infty \int_{-\infty}^\infty \int_{-\infty}^\infty d^3\kappa \exp(i\mathbf{\kappa}\mathbf{r}) F_z(\kappa), \quad (9)$$

where

$$F_z(\kappa) = \frac{1}{4\pi} \frac{55}{27} \frac{C}{\Gamma(1/3)} \varepsilon_T^{2/3} |\kappa|^{-11/3} \left(1 - \frac{\kappa_z^2}{|\kappa|^2}\right) \quad (10)$$

is the three-dimensional spectrum of the velocity radial component,<sup>18</sup>  $\Gamma(x)$  is the gamma function,  $C \approx 2$  is the Kolmogorov's constant;  $\varepsilon_T$  is the dissipation rate of turbulent energy;  $\kappa = \{\kappa_z, \kappa_x, \kappa_y\}$ . By substituting (9) into (8) we obtain

$$S_D(f) = 2 \int_{-\infty}^{+\infty} d\tau e^{-i2\pi f \tau} \int_{-\infty}^\infty \int_{-\infty}^\infty \int_{-\infty}^\infty d\kappa_z d\kappa_x d\kappa_y \exp\{i\kappa_z \langle V_z \rangle \tau + \\ + i\kappa_x \langle V_x \rangle \tau\} F_z(\kappa_z, \kappa_x, \kappa_y) H(\kappa_z) + S_n, \quad (11)$$

where

$$H(\kappa_z) = \left| \int_0^\infty dz Q_s(z) e^{i\kappa_z z} \right|^2 \tag{12}$$

is the transfer function of the spatial low-frequency filter. Taking into account the condition  $ka_0^2 \gg R$  for  $H(\kappa_z)$  from Eqs. (2), (3), and (12) we have

$$H(\kappa_z) = \exp \left\{ -\frac{2}{\pi} \Delta z |\kappa_z| \right\}. \tag{13}$$

Let us introduce in Eq. (11) a new integration variables:

$$\kappa'_z = \kappa_z \cos \gamma + \kappa_r \sin \gamma, \quad \xi = (\kappa_z \cos \gamma - \kappa_r \sin \gamma)U / (2\pi f),$$

where  $\gamma = \arccos(\langle V_z \rangle / U)$  is the angle between wind direction and propagation axis of the sounding beam  $z$ ;  $U = |\langle \mathbf{V} \rangle|$  is the modulus of wind mean velocity vector. Using the formulas (10) and (13) in Eq. (11) we integrate over the variables  $\tau$ ,  $\kappa'_z$  and  $\kappa_y$ . As a result we finally obtain

$$S_D(f) = S_z(f) H(f) + S_n, \tag{14}$$

where

$$S_z(f) = C_1 \left( 1 + \frac{1}{3} \sin^2 \gamma \right) \varepsilon_T^{2/3} U^{2/3} f^{-5/3} \tag{15}$$

is the temporal spectrum of  $z$ -component of the wind velocity at a fixed point ( $z = R$ ),  $C_1 = 2C / [3\Gamma(1/3)(2\pi)^{2/3}] \approx 0.15$ ,

$$H(f) = C_2 \left( 1 + \frac{1}{3} \sin^2 \gamma \right)^{-1} \int_{-\infty}^{+\infty} d\xi (1 + \xi^2)^{-4/3} \times \\ \times \left[ 1 - \frac{8}{11} \frac{(\cos \gamma - x \sin \gamma)^2}{1 + x^2} \right] \times \\ \times \exp \left\{ -\frac{4 \Delta z f}{U} |\cos \gamma - x \sin \gamma| \right\} \tag{16}$$

is the transfer function of temporal low-frequency filter,  $C_2 = (55/27)[\Gamma(1/3)/\Gamma(11/6)] / (4\sqrt{\pi})$ .

In the particular cases it is possible to calculate the integral in (16) analytically. So, for  $\Delta z \rightarrow 0$  the function  $H(f) \rightarrow 1$ . In the case when the directions of beam propagation and mean wind coincide ( $\gamma = 0$ ) from Eq. (16) we have

$$H(f) = \exp\{-4 \Delta z f / U\}. \tag{17}$$

Under the condition

$$(4 \Delta z |\sin \gamma| / U) f \gg 1 \tag{18}$$

the main contribution to the integral (16) is caused by small area about the point  $\xi_m = \cotan \gamma$ , boundaries of this area are determined by a sharp decrease of the exponent when moving off from  $\xi_m$ . Therefore in (16) for the factor before the exponent it can be assumed

that  $\xi = \xi_m$  and integration can be performed. As a result we obtain

$$H(f) = C_2 \left( 1 + \frac{1}{3} \sin^2 \gamma \right)^{-1} \frac{1}{2} \frac{U |\sin \gamma|^{5/3}}{\Delta z f}. \tag{19}$$

Thus, in the given case for the velocity spectrum measured with the Doppler lidar we have

$$S_D(f) = C_3 \varepsilon_T^{2/3} |\langle V_x \rangle|^{5/3} \frac{1}{\Delta z} f^{-8/3} + S_n, \tag{20}$$

where  $C_3 = C_1 C_2 / 2 \approx 0.06$ ;  $\langle V_x \rangle = U \sin \gamma$ . It follows from Eq. (20) that in the absence of noise ( $S_n = 0$ ) the spectrum of Doppler velocity under the condition (18) is proportional to  $f^{-8/3}$ .

### EXPERIMENT

The measurements were carried out using a CO<sub>2</sub> cw Doppler lidar of the Institute for Optoelectronics near Oberpfaffenhofen (Germany) in September 1995. The container with the lidar was installed on an open platform. There are three- and four-storeyed buildings (which are about 100 m from the container) on the one side of the platform only. Behind this buildings there is a forest. Run of Doppler lidar measurements was carried out for different sounding geometry (height and dimension of the volume sounded changed) and dynamic turbulence intensity.

Before the start of every single measurement the angles of location  $\varphi$  and propagation direction  $\theta$  of laser beam which was focused at a given distance  $R$  were adjusted with a scanning device. During the measurement session of duration  $T$  the Doppler spectra were recorded with the frequency 20 Hz and integral averaging period  $t_0 = 0.05$  s. When the session finished the radial wind velocity  $V_D(t_i)$  (where  $t_i = it_0$ ,  $i = 0, 1, 2, \dots, N (Nt_0 = T)$ ) was estimated from every Doppler spectrum. The data obtained were used to calculate the spectrum of turbulent fluctuations of the velocity  $\hat{S}_D(f_k)$ , where  $f_k = k\Delta f$ ,  $k = 0, 1, 2, \dots, N/2$ ;  $\Delta f = 1/T$ , with the fast Fourier transform code. Smoothing (averaging) of spectrum estimates was performed by the rectangular spectral window. We estimated the mean wind velocity  $U$  and direction  $\gamma$  from additional lidar measurements with the laser beam conical scanning.<sup>1</sup>

Results of processing measurements carried out on September 27, 1995 from 14:30 to 16:00 are presented below. Weather conditions during this time were characterized by a strong turbulization of air flow. At the height  $h = 200$  m the wind velocity reached 16 m/s. The sky was covered with low clouds, owing to that an additional peak connected with reflection of sounding radiation from a cloud appeared in the measured Doppler spectra at an increased sounding height  $h$  up to 300 m. Therefore, in the given experiment we were limited to the maximum height  $h = 200$  m. Note, that the cloud motion velocity exceeded the wind velocity at the height  $h = 200$  m by a factor of 1.5.

The measurements were carried out at the heights 10; 25; 50; 100, and 200 m. The corresponding values of longitudinal size of the volume sounded were  $\Delta z = 2.3; 4.5; 9.2; 30; \text{ and } 100$  m. For large  $\Delta z$  the azimuth angle  $\theta$  was chosen in such a way that the angle  $\gamma$  was maximal, hereby we got the largest values of the side wind velocity  $\langle V_x \rangle$  to compare the measurement results on the spectrum  $S_D$  with the asymptotic calculations.<sup>20</sup> Note, that for  $\Delta z = 100$  m ( $h = 200$  m) the integral longitudinal scale of correlation of radial wind velocity  $L_V$  is compared with  $\Delta z$ .

The estimates of smoothed values of the velocity fluctuation spectra (with averaging over 24 statistic degrees of freedom) are shown by points in Fig. 1. One can see that the values of spectra obtained from the Doppler lidar data decrease with the frequency  $f$  more rapidly that it follows from the “ $-5/3$ ” Kolmogorov-Obukhov’s power law (dashed lines 1). In the experiment we had various values of the signal-to-noise ratio that was observed easily during the measurements from the obtained Doppler spectra. It affected the amplitudes of noise level  $S_n$  in the velocity spectra  $S_D$  presented in Fig. 1. The data on  $U$  and  $\gamma$  are shown in Table I at different heights.

TABLE I.

$h, \text{ m}$	10	25	50	100	200
$\Delta z, \text{ m}$	2.3	4.5	9.2	30	100
$U, \text{ m/s}$	5.2	6.3	8.7	13.5	15.6
$\gamma, \text{ deg.}$	13	27	34	60	75

The comparison of calculations by formula (14), with an arbitrary  $\varepsilon_T$  and  $S_n = 0$ , with the experimental spectra in the low-frequency region where the spectrum noise component can be neglected shows that qualitatively these spectra coincide quite well. Proceeding from this we found the estimates of dissipation rate of turbulent energy  $\varepsilon_T$  by the formula

$$\varepsilon_T = \left[ \frac{1}{n_2 + 1 - n_1} \sum_{i=n_1}^{n_2} \frac{\hat{S}_D(f_i)}{A(f_i)} \right]^{3/2}, \tag{21}$$

where  $A(f_i) = S_z(f_i)H(f_i)/\varepsilon_T^{2/3}$  and  $S_z(f_i)$  and  $H(f_i)$  were calculated by the expressions (15) and (16), respectively. Here the frequency  $f_{n_1} = n_1/T$  is the low boundary of inertial interval and satisfies the condition  $f_{n_1} > U/L_V$ . The number of spectrum channel  $n_2$  was chosen in such a way that it corresponds to the highest frequency  $f_{n_2} = n_2/T$  when the noise contribution into the spectrum  $S_D$  remains yet negligible. The values  $S_n$  were calculated by the formula

$$S_n = \frac{1}{N/2 + 1 - n_3} \sum_{i=n_3}^{N/2} \hat{S}_D(f_i), \tag{22}$$

where  $n_3$  corresponds to the frequency  $f_{n_3} = n_3/T > f_{n_2}$  when the main contribution into the measured spectrum comes from noise.

Using the values  $\varepsilon_T$  and  $S_n$  obtained from the experimental data the calculations  $S_D(f)$  were performed by formula (14). The calculations are presented by solid lines in Fig. 1. The calculations  $S_z(f)$  by formula (15) and the noise spectra  $S_D$  (dashed lines 1 and 2) are presented in the figure also. The dashed line 3 is the result of  $S_D$  calculation by formula (14) for  $S_n = 0$ . One can see from the data presented that the theory (solid lines) and experiment (points) agree quite well. The spread of experimental points is within the estimated error of smoothed spectra (the relative error is  $\sim 30\%$ ).

Figure 2 shows the height profile of the dissipation rate of turbulent energy  $\varepsilon_T$  reconstructed by the data presented in Fig. 1. The height dependence  $\varepsilon_T(h)$  is analogous to the results of measurements obtained at the meteorological mast IEM in Obninsk under neutral stratification and strong wind. However, the magnitudes  $\varepsilon_T$  obtained by us exceed, by the absolute value, more then twice the corresponding data from Ref. 20. Possibly, it is connected with the difference in the values of underlying surface roughness parameter in our experiment and in the area of the meteorological mast IEM, or might be the result of specific weather conditions during the measurements described above.

It follows from the above said that the spectrum of wind velocity measured with the Doppler lidar is the sum of the spectrum of radial wind velocity averaged over lidar volume and noise spectrum. To separate useful component of the spectrum measured we carry out a correction of the smoothed spectrum by simple subtraction from it of the regular noise component  $S_n$ . Use of this procedure can be justified only for the frequencies  $f$  which satisfy the condition  $S_D(f) - S_n \gg \sigma_n^2$ , where  $\sigma_n^2 = 2S_n^2/n_d$  is the variance of the noise component of spectrum averaged at  $n_d$  statistical degrees of freedom.

The corrected spectrum values are denoted by points in Fig. 3. The initial data correspond to Fig. 1e ( $h = 200$  m,  $\Delta z = 100$  m) and satisfy the condition (18) over the entire range of the frequencies considered. The corrected spectrum must coincide with the calculation by formula (20) for  $S_n = 0$  presented in the figure as a solid line. One can see that the experimental data are described by the dependence  $S_D(f) \sim f^{-8/3}$  with a good accuracy. The calculated data on  $S_z(f) \sim f^{-5/3}$  by the formula (15) are shown by the dashed line in the figure. Already at low frequencies  $f \sim 0.3$  Hz the values of the lidar spectrum are less by an order of magnitude than corresponding velocity spectrum values measured with a non-inertial point device owing to the strong spatial averaging over the volume sounded ( $\Delta z \sim 100$  m  $\sim L_V$ ).

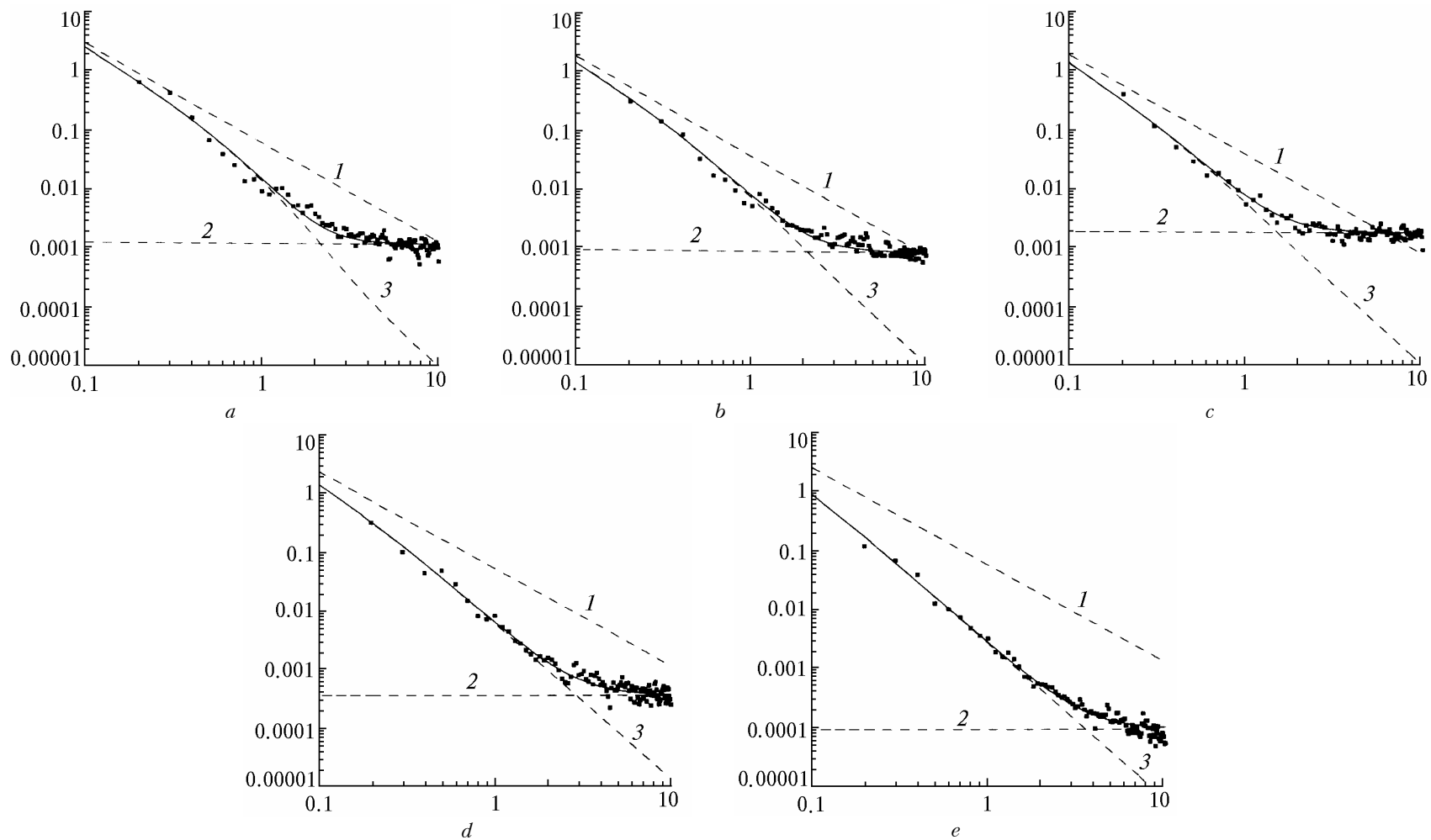


FIG. 1. Spectra  $S_D$  of wind velocity measured with a Doppler lidar (axis of ordinates,  $m^2/s$ ) at the heights  $h = 10$  m (a), 25 m (b), 50 m (c), 100 m (d), and 200 m (e) (frequency  $f$ , Hz, is along the abscissa). Points are the experiment, solid curve is the theory (calculation by formula (14)), dashed curves 1, 2, 3 are the calculations of spectrum by formula (15), the spectrum of noise component of Doppler velocity, and results of spectrum calculations by formula (14) for  $S_n = 0$ , respectively.

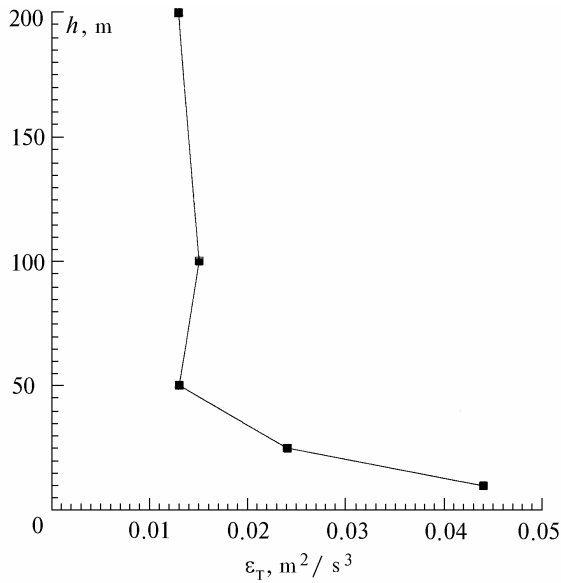


FIG. 2. Height profile of the dissipation rate of turbulence energy retrieved from the data of Doppler lidar.

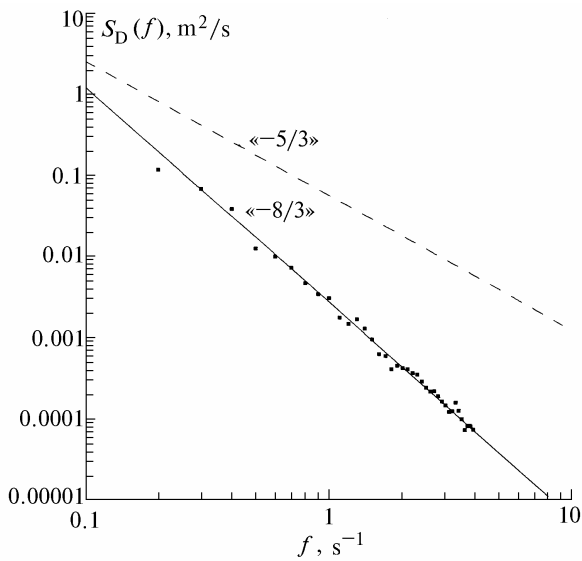


FIG. 3. The spectrum of wind velocity measured with the Doppler lidar at the height  $h = 200$  m; points are the experiment, dashed line is the calculation by formula (15); solid line - calculations by formula (20) for  $S_n = 0$ .

The results presented above relate to the cases when during the measurements either longitudinal size of lidar volume  $\Delta z$  was small or quite strong side wind  $\langle V_x \rangle = U \sin \gamma$  occurred that provided applicability of the theory considered in the present paper to analyze the experimental data.

A question arises: on how the spectra of velocity measured at large  $\Delta z$  and arbitrary values  $\langle V_x \rangle$  (angles  $\gamma$ ) behave? To answer this question, the most typical data obtained for the sounding beam propagation

directions coincident with mean wind ( $\gamma \approx 0$ , horizontal path,  $h = 3$  m) were selected from the results measured on 26.09.95. In this case the longitudinal size of lidar volume  $\Delta z$  was 218 m that considerably exceeds the scale of wind velocity correlation  $L_V$  at the height  $h = 3$  m. The measurements were carried out at a moderate wind  $U \sim 3.5$  m/s and very high signal-to-noise ratio.

The results of estimate of the smoothed spectrum of velocity obtained from the data of this experiment are presented as points in Fig. 4. Analysis of the spectrum shows that it does not obey the theoretical relationships derived in this paper. Under the assumption that the spectrum ensemble averaged is described by the power law, i.e.  $S_D(f) \sim f^\nu$ , from the dependence of the logarithm of non-smoothed spectrum  $\ln \hat{S}_D$  on the logarithm of frequency  $\ln f$  the power index  $\nu$  of the experimental spectra slope was determined with the least squares method. This index is approximately equal  $-2$ . The power dependence obtained is shown by solid line in Fig. 4.

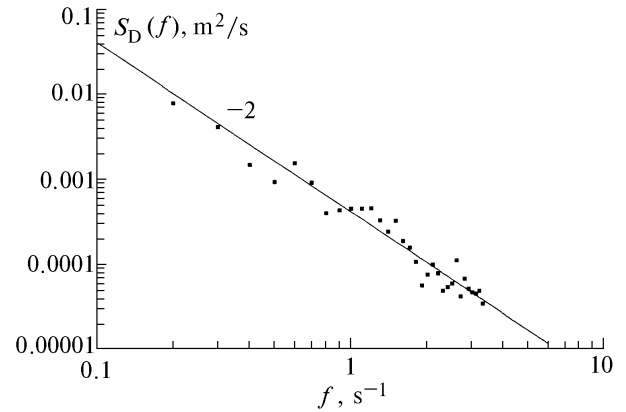


FIG. 4. The spectrum of wind velocity measured with the Doppler lidar for large longitudinal size of the volume sounded and coincidence of directions of laser beam propagation and wind: points are the experiment, solid line is the result of adjustment of the measured data to power dependence of spectrum on frequency.

Analysis of the results of other lidar sessions of measurements showed that the velocity spectra obtained for different heights  $h$ , when  $\Delta z \geq L_V$  and  $\gamma < 15^\circ$ , also have the power dependence  $S_D(f) \sim f^{-2}$ . Note, that, as the experimental data show, the

$$\text{spectrum of the Doppler signal } I_D(t) \sim \int_0^\infty dz Q_s(z) \beta_\pi(z, t),$$

which is proportional to the backscattering coefficient averaged over the volume sounded (particle concentration) has similar dependence.

The most probable cause of the discrepancy between the theory developed and the experiment results in Fig. 4, in our opinion, is the use of the

hypothesis of "frozen" turbulence (formula (7)). In the considered case to describe the spectrum of velocity measured with a Doppler lidar correctly it is necessary to take into account a side removal of aerosol particles from the volume sounded by the turbulent vortices of different scales (fluctuations of transverse components of wind velocity vector) and evolution of this vortices in time (turbulent diffusion).

### CONCLUSION

Thus, it follows from the results presented that when the condition of the Taylor hypothesis of "frozen" turbulence holds the temporal spectrum of wind velocity measured with a Doppler lidar for large longitudinal size of lidar volume has an essential difference in the inertial interval from turbulence spectrum measured with a low-inertial point device and is proportional to  $f^{-8/3}$ . This is a result of essential spatial averaging of fluctuations of radial wind velocity over the volume sounded.

The experimental spectrum of velocity measured with the Doppler lidar at coincident directions of the sounding beam axis and mean wind and large sounding volume, when the conditions of the Taylor hypothesis is broken, differs from the spectrum measured at a point also, but has a dependent of type  $S_D = \alpha f^{-2}$  where  $\alpha$  is the proportional<sup>2</sup> coefficient having a dimension of dissipation rate of the turbulent energy,  $m^2/s^3$ . Explanation of these results is possible only on the basis of a theory using adequate model for spatial temporal correlation function of the radial component of wind velocity.

### ACKNOWLEDGMENT

The paper is supported by the Russian Foundation of Fundamental Research (project N 94-05-16601-a).

### REFERENCES

1. F. Kopp, R.L. Schweisow, and Ch.J. Werner, *J. Climate Appl. Meteorol.* **23**, 148–154 (1984).
2. F.F. Hall, R.M. Huffaker, R.M. Hardesty, M.E. Jakson, T.R. Lawrence, M.J. Post, R.A. Richter, and B.F. Weber, *Appl. Opt.* **23**, No. 15, 2503–2506 (1984).
3. J.G. Hawley, R. Tang, S.W. Henderson, C.P. Hale, M.J. Kavaya, and D. Moerder, *Appl. Opt.* **32**, No. 24, 4557–4568 (1983).
4. F. Kopp, Ch. Werner, R. Haring, V.A. Banakh, I.N. Smalikho, and H. Kambezidis, *Contribution to Atmospheric Physics* **67**, No. 4, 269–286 (1994).
5. V.A. Banakh, I.N. Smalikho, F. Kopp, and Ch. Werner, *Appl. Opt.* **34**, No. 12, 2055–2067 (1995).
6. V.M. Gordienko, A.A. Kormakov, L.A. Kosovsky, N.N. Kurochkin, G.A. Pogosov, A.V. Priezzhev, and Y.Y. Putivskii, *Optical Engineering* **33**, No. 10, 3206–3213 (1994).
7. R.J. Keeler, R.J. Serafin, R.L. Schwiesow, D.H. Lenshow, J.M. Vaughan, and A.A. Woodfield, *Journ. Atmos. Oceanic Technol.* **4**, 113–127 (1987).
8. R.G. Frehlich, S.M. Hannon, and S.W. Henderson, *Journ. Atmos. Oceanic Technol.* **11**, No. 6, 1517–1528 (1994).
9. Tzvi Cal-Chen, Mei Xu, and W.L. Eberhard, *J. Geophys. Research* **97**, No. D17, 18409–18423 (1992).
10. G.M. Ancellet, R.I. Menzies, and V.B. Grant, *Journ. Atmos. Oceanic Technol.* **6**, No. 1, 50–58 (1989).
11. S.M. Hannon, J.A. Thomson, S.W. Henderson, and R.M. Huffaker, *Air Traffic Control Technologies. Proc. SPIE* **2464**, 94–102. (1995).
12. V.A. Banakh, Ch. Werner, N.N. Kerkis, F. Kopp, and I.N. Smalikho, *Atmos. Oceanic Opt.* **8**, No. 12, 955–959 (1995).
13. T.R. Lawrence, D.J. Wilson, C.E. Craver, I.P. Jones, R.M. Huffaker, and J.A. Thomson, *Rev. Sci. Instrum.* **43**, No. 3, 512–518 (1972).
14. C.M. Sonnenschein and F.A. Horrigan, *Appl. Opt.* **10**, No. 7, 1600–1604 (1971).
15. V.A. Banakh, I.N. Smalikho, and Ch. Werner, *Lidar Techniques for Remote Sensing, Proc. SPIE* **2310**, 224–232 (1994).
16. I.N. Smalikho, *Atmos. Oceanic Opt.* **8**, No. 10, 788–793 (1995).
17. I.L. Lumley and H.A. Panofsky, *The Structure of Atmospheric Turbulence* (Interscience, New York, 1964).
18. A.S. Monin and A.M. Yaglom, *Statistical Hydromechanics*. Part II. (Nauka, Moscow, 1967) 720 pp.
19. A.C. Gurvich, *Izv. Akad. Nauk SSSR, Fiz. Atmos. Okeana* **16**, No. 4, 345–354. (1980).
20. Z.I. Volkovitskaya and V.P. Ivanov, *Izv. Akad. Nauk SSSR, Fiz. Atmos. Okeana* **6**, No. 5, 435–444 (1970).